EV Integration-Oriented DC Conversion of AC Low-Voltage Distribution Networks and the Associated Adaptive Control Strategy

Bo Zhang, Wei Tang*, *Member*, *IEEE*, Jun Liang, *Senior Member*, *IEEE*, Lu Zhang, *Member*, *IEEE*, Chunxue Zhao

***Abstract*- Driven by carbon-neutral targets and transportation electrification, the widespread use of electric vehicles (EVs) has become an irreversible trend. However, low-voltage distribution networks (LVDNs) can face several challenges under the high-penetration EV integration, including overloads, voltage violations and unbalance issues. In this paper, an EV integration-oriented DC conversion scheme and the associated adaptive control method for LVDNs is proposed, aiming at releasing more capacity for EVs and collaborative improvement of the above issues caused by EV charging. Based on analyzing the influence of different charging piles connected to the AC and DC LVDNs, a DC conversion scheme for three-phase four-wire LVDNs under high-penetration EVs is proposed. The voltage source converter (VSC) control strategies aimed at alleviating the overload of the DTs, voltage violations, and three-phase unbalance are designed separately based on the modified three-phase four-wire voltage sensitivity. Then, a coordinated adaptive control strategy of on-load tap changer and VSCs is proposed considering the simultaneous occurrence of multiple power quality issues in hybrid AC/DC LVDNs. Case study verifies the effectiveness of the proposed DC conversion and adaptive control methods, by which the maximum EV penetration of the hybrid AC/DC LVDN is increased from 85% to 215% compared with the AC LVDN.**

***Index Terms*-Low-voltage distribution network (LVDN), electric vehicle (EV), transportation electrification, hybrid AC/DC, voltage source converter (VSC), adaptive control.**

I. Introduction

In response to carbon-neutral targets for global temperature control, transportation electrification has become an irreversible trend [1], and electric vehicles (EVs) are an important part of this electrification [2]. The number of EVs worldwide has increased rapidly in recent years, and reached 16.5 million in 2021 according to the "Global EV Outlook 2022" of International Energy Agency. However, low-voltage distribution networks (LVDNs) can face several challenges with the integration of high-penetration EVs [3], [4]. For instance, the single-phase integration of AC charging piles can further aggravate unbalance issues [5]. The increasing use of DC charging piles can lead to voltage violations (undervoltage) and overloads of distribution transformers (DTs) and lines [6]. Moreover, the randomness of the EV charging load makes it more difficult to address the above-mentioned power quality issues due to the limited control capability of AC LVDNs [7].

In order to address the impacts caused by high-penetration EVs in three-phase four-wire AC LVDNs, various studies have been conducted [8]-[12]. Building dedicated DTs and lines for EV charging piles can alleviate these problems [8], [9]. However, the feasibility of this high-investment solution is limited as the unbalance caused by AC charging piles can still exist. Some reactive power controllable devices, such as static var generator and shunt capacitors, can flexibly manage reactive power and thereby control the voltage in LVDNs [10], [11]. However, the regulation of reactive power can only improve the voltage quality without providing active power support for EV charging. Distribution transformers equipped with on-load tap changers (OLTCs) can be used to regulate voltage violation issues [12]. However, its applicability is limited as the OLTC cannot be operated frequently, while the overloads and unbalance issues cannot be solved by adjusting the taps. Besides, power transfer between low-voltage lines with complementary characteristics might be a possible way to deal with the overloads and voltage violations, however, it is not suitable for LVDNs as their topologies are normally radial.

Compared with the solutions that solely based on AC LVDNs [8]-[12], DC technology has the potential to address these issues caused by EV integration. In distribution networks, DC technology has been widely used to increase the power transfer capacities and improve power quality, thus makes it more suitable for the integration of DC piles [13]-[15]. In a hybrid AC/DC distribution network, power flow between AC and DC lines can be rescheduled flexibly through three-phase power regulation of voltage source converters (VSCs) [16], [17], which ensures a strong capability in regulating both the voltage and power for EV integration.

Converting existing AC lines to DC operation is a techno-economic solution to achieve a hybrid AC/DC system, where the related DC conversion schemes for medium-voltage distribution networks (MVDNs) have been proposed in [18]

This work was supported by The National Key Research and Development Program of China (2019YFE0118400).

Bo Zhang, Wei Tang (corresponding author), Lu Zhang, and Chunxue Zhao are with China Agricultural University, Beijing 100083, China (e-mail: zhangbo1223@foxmail.com, wei_tang@cau.edu.cn, zhanglu1@cau.edu.cn, caustuzcx@cau.edu.cn). Jun Liang is with Cardiff University, Cardiff CF 24 3AA, U.K. (e-mail: LiangJ1@cardiff.ac.uk).

and [19]. However, as the MVDN is a three-phase three-wire topology that differs from the three-phase four-wire configuration of LVDN, the existing DC conversion methods designed for MVDNs are not suitable for LVDNs to fully utilize their line capacity. In addition, the AC and DC charging piles for EVs will result in different power quality issues, and the required power supply topologies need to be adjusted accordingly. However, such application scenarios have not been considered in the existing DC conversion methods. As a result, it is necessary to design an effective DC conversion method for three-phase four-line LVDNs considering EV integration.

Besides the DC conversion methods, the existing control schemes for hybrid AC/DC MVDNs [20], [21] are also not applicable for LVDNs due to their innate topological difference. Ref. [22] proposes a coordinated voltage control scheme to regulate voltage in a hybrid AC/DC distribution network, in which the OLTC, shunt capacitors, and distributed generators are coordinated adjusted with the microgrids. Reference [23] proposes an improved method through the zero-sequence voltage injection in the converters to keep balancing the three-phase grid currents and DC capacitor voltages in the DC side. An energy management method is proposed for hybrid AC/DC microgrid in [24], to deal with the impact of uncertainty on the power interaction. An accurately improved sensitivity calculation method based on the ABCD parameters for hybrid AC/DC LVDNs is proposed in [25]. It is still challenging to design the coordinated control scheme for hybrid AC/DC LVDNs under EV integration. More specifically, the whole control method must incorporate not only the control objectives of unbalance, overloads, and voltage violations of hybrid AC/DC LVDNs under EV integration, but also the system-level control considering the lack of communication, i.e., in LVDCs, the coordination among multiple lines, phases, and control objectives must be achieved using limited communication. In addition, although the coordination among multiple lines and phases via VSCs can help realize the load transfer between AC and DC lines as well as mitigating the unbalance problems of AC networks, this may lead to the aggravation of other issues without considering the coordination of multiple control objectives.

To address the issues concerning EV-integrated LVDNs from a DC perspective, this paper proposes a DC conversion scheme and its associated adaptive control strategy, which can release more capacity for EV integration and alleviate the overloads, unbalance, and voltage violation problems caused by the AC and DC charging piles effectively. The main contributions of this paper are summarized as follows:

1) Propose a novel DC conversion scheme for three-phase four-wire LVDNs with high-penetration EVs. Firstly, the power transfer capacities, voltage drops and power losses of the AC and DC LVDNs are quantitatively analyzed, considering the influences of EV charging loads. Then, a DC conversion scheme for releasing more capacity for EV integration is proposed, including both the topology of hybrid AC/DC LVDNs and VSC configurations.
2) Propose a coordinated control method for hybrid AC/DC LVDNs with high-penetration EVs. Firstly, the control strategies aimed at alleviating the overload of the DTs, voltage violations, and three-phase unbalance are designed separately based on the modified three-phase four-wire voltage sensitivity. Then, a coordinated control strategy of VSC and OLTC is proposed considering the simultaneous occurrence of multiple power quality issues in hybrid AC/DC LVDNs.

II. DC Conversion Scheme of LVDN Considering the Influence of EV Charging Piles

A. Influence Analysis of AC and DC EV Charging Piles

In AC LVDNs with EV integration, the EV charging piles can induce the unbalance, overload, and voltage violation problems. Therefore, their influence on the system needs to be analyzed in detail before designing the corresponding DC conversion scheme. The existing EV charging piles include DC and AC charging piles, which are also called fast-charging and slow-charging piles, respectively [26].

For AC charging piles, the input and output voltages are both AC. The EV on-board converter, which is usually small in volume (7 kW is common), is used to charge the battery. As the AC charging piles are generally located in residential areas, their charging load characteristics are regular, i.e., usually charging at night.

For DC charging piles in AC LVDNs, the input voltage is AC while the output voltage is DC. Therefore, both AC-DC and DC-DC converters are included in DC charging piles, and the charging power is relatively larger than AC, e.g., 40 - 200 kW. The DC piles are mostly located in commercial and office areas to meet users' short-term charging demands. Therefore, the load characteristics of the DC piles are irregular, as EV users may charge at any time of the day.

When AC and DC charging piles are connected to the AC lines, as shown in Fig. 1, it may cause overloads, undervoltage, and unbalance issues. More specifically, when AC charging piles are connected to the AC 220 V distribution lines in LVDNs, the three-phase unbalance issue can be aggravated. Besides, the integration of DC charging piles can lead to overloads of DTs and lines. As for the undervoltage issues caused by AC piles, they can be improved by adjusting the OLTC since they are regular and long-lasting. However, as the undervoltage issues caused by the DC pile are short-term and frequent, they cannot be effectively addressed by the OLTC, as it cannot be operated frequently. In addition, the problems of overloads and unbalance cannot be solved by adjusting the taps of OLTC either.

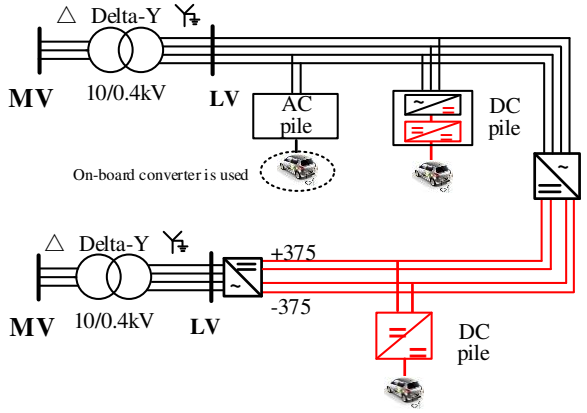

Fig. 1. Topology of a hybrid AC/DC LVDN with AC and DC charging piles.

In order to release more capacity for EV integration and alleviate the above-mentioned issues caused by AC and DC charging piles, a DC conversion scheme is proposed. When some low-voltage AC lines in AC LVDNs are converted to DC operations, the DC charging piles can be directly connected to the DC lines, thus the AC/DC converter is no longer needed, as shown in Fig. 1. The maximum power transfer capacity and voltage drop of the converted DC line have changed compared with the original AC line. The maximum power transfer capacities of the AC and DC LVDN shown in Fig. 1 can be expressed as follow:

$$\begin{cases} P_{\max}^{AC} = \sqrt{3} U_{AC}^{\text{rated}} I_{AC} \cos\varphi \\ P_{\max}^{DC} = 4 U_{DC}^{\text{rated}} I_{DC} \end{cases} \tag{1}$$

where U_{DC}^{rated} and U_{AC}^{rated} are the rated voltage of the DC and AC lines, I_{DC} and I_{AC} are maximum currents, φ is the phase difference between voltage and current.

For the given EV charging load P_l and Q_l, the voltage drops of the AC and DC LVDN shown in Fig. 1 are:

$$\begin{cases} \Delta U_{AC} = (P_l \cdot r_{AC} + Q_l \cdot x_{AC}) / U_{AC}^{\text{rated}} \\ \Delta U_{\text{DC}} = P_l / 4 U_{DC}^{\text{rated}} \cdot r_{\text{DC}} \end{cases} \tag{2}$$

where r_{DC} and r_{AC} are resistances.

Power losses of the AC LVDN under the EV charging load P_l and Q_l are expressed in equation (3):

$$P_{loss}^{AC} = \frac{P_l^2 + Q_l^2}{U_{AC}^2} \cdot r_{AC} \tag{3}$$

Power losses of the DC LVDN carrying the same power Pl are expressed in equation (4):

$$P_{loss}^{DC} = \left(\frac{P_l}{2U_{DC}} \right)^2 \cdot r_{DC} = \frac{P_l^2}{4U_{DC}^2} r_{DC} \tag{4}$$

According to equations (1)-(4) and the relationship of current and resistance of DC conversion [18], i.e., r_{DC} =0.98r_{AC}, I_{DC} =1.01I_{AC}, the ratio of power transfer capacity, voltage drop and power losses of the DC and AC can be obtained as:

$$\begin{cases} P_{\max}^{DC} / P_{\max}^{AC} = 2.588 \\ \Delta U_{\text{DC}} / \Delta U_{AC} = 0.234 \\ P_{loss}^{DC} / P_{loss}^{AC} = 0.167 \end{cases} \tag{5}$$

Therefore, the undervoltage issues and overloads caused by DC charging piles can be alleviated by the DC conversion due to the increased power transfer capacity and smaller voltage drop in DC system. Moreover, the converted DC lines can be interconnected with other AC lines, then unbalance issues caused by AC charging piles can be further improved by regulating the three-phase power of the VSCs.

Based on the above analysis, it is recommended that the AC charging piles are still connected to the AC lines, while the DC charging piles can be connected to the DC lines in hybrid AC/DC LVDNs.

B. DC Conversion Scheme of LVDNs with EV Integration

In this section, the DC conversion scheme of LVDNs with EV integration is presented, including both the topologies of hybrid AC/DC LVDNs and VSC configurations.

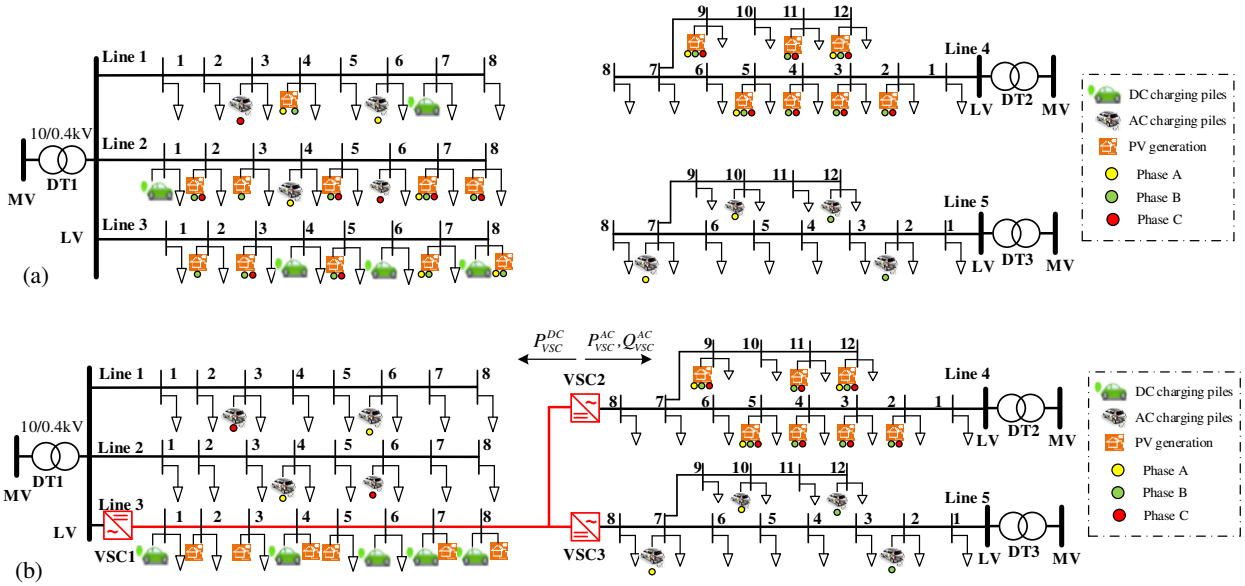

Fig. 2. Topology of LVDNs with charging piles. (a) AC LVDN; (b) hybrid AC/DC LVDN.

The proposed DC conversion scheme is operated by converting the AC line that equipped with the largest amount of DC charging piles into DC operation, and the converted DC line can also be interconnected with other AC lines. Take the LVDN with three adjacent distribution areas and high penetration charging piles as in Fig. 2 (a) to illustrate the proposed DC conversion method. As shown in Fig. 2 (a), most of the DC charging piles are connected to Line 3, thus Line 3 is converted into DC operation, as shown in Fig. 2 (b). The adjacent DC charging piles in other lines can be relocated to the converted Line 3, while the other farther ones remain unchanged. Besides, three distribution areas are interconnected by VSC2 and VSC3 in Fig. 2 (b), which form a hybrid AC/DC LVDN. After the DC conversion, although the converters for AC loads are still required, the AC/DC converters for the DC charging piles are saved. Therefore, more capacities are released for EV integration and the power quality issues are alleviated by the proposed method.

After the hybrid AC/DC LVDN topology is determined by DC conversion, the configuration of VSCs also needs further analysis, since the VSC configuration can affect the transfer capacity, voltage drop, reliability and investment.

As LVDNs are generally constructed with a three-phase four-wire configuration that is different from the three-phase three-wire MVDNs, the DC configurations converted from LV AC lines can be asymmetric monopoles, symmetric monopoles, parallel operation monopoles, and bipolar configurations. If the AC LVDN is converted to the asymmetric monopole as shown in Fig. 3 (a), the four wires will combine as a DC conductor, and an extra conductor is needed as the dedicated metallic return. If the AC LVDN is converted to the symmetric monopole as shown in Fig. 3 (b), the four wires in the AC LVDN are utilized as the positive and negative poles, respectively. If the AC LVDN is converted to the parallel operation monopoles as shown in Fig. 3 (c), two VSCs and the four existing AC wires can all be utilized, which is more reliable than the monopole configuration, as a failure in one link will not affect the operation of the other link. If the AC LVDN is converted to the bipolar configuration as shown in Fig. 3 (d), only three of the four existing AC wires are used as the positive pole, negative DC pole and neutral wire.

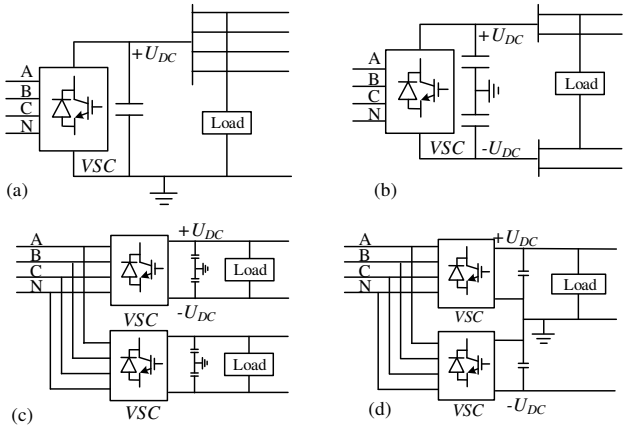

Fig. 3. DC link configurations converted from AC lines. (a) Asymmetric monopole with a dedicated metallic return; (b) symmetric monopole; (c) parallel operation monopoles; (d) rigid bipolar configuration.

To evaluate the four VSC configurations in Fig. 3, their maximum power transfer capacity, voltage drop and power losses can be calculated according to the relationship of the voltage, current and resistance before and after the DC conversion. Table I shows the maximum power transfer capacity, voltage drop, power losses, reliability and investment of different DC configurations compared with the AC LVDN. As shown in Table I, the parallel operation monopoles have the same power transfer capacity, voltage drop and power loss as the symmetric monopole, with the high-level reliability and medium-level investment cost due to the two VSCs exist. Considering that the DC charging piles are generally installed in urban areas where four-core underground cables are widely used, it is thus recommended to adopt the parallel operation monopole shown in Fig. 3 (c) for hybrid AC/DC LVDN with EV charging. In this way, the existing four wires of underground cables can be fully utilized, and the power supply capacity, voltage drop, power loss, and reliability of this configuration are all equal to or better than those of the other three configurations.

TABLE I
COMPARISONS OF VARIOUS CONFIGURATIONS

Configurations	$\frac{P_{\max}^{DC}}{P_{\max}^{AC}}$	$\frac{\Delta U_{DC}}{\Delta U_{AC}}$	$\frac{P_{loss}^{DC}}{P_{loss}^{AC}}$	Reliability	Investment
Asymmetric monopole	2.558	0.234	0.334	Low	High (a new line and single VSC)
Symmetric monopole	2.558	0.234	0.167	Medium	Low (single VSC)
Parallel operation monopoles	2.558	0.234	0.167	High	Medium (two VSCs)
Bipolar configuration	1.279	0.468	0.334	High	Medium (two VSCs)

III. CONTROL METHOD FOR HYBRID LVDNS WITH INTEGRATION OF EVS

As mentioned previously, although the OLTC is suitable for improving the voltage violations on long-time scale such as undervoltage issues caused by AC piles, it cannot be operated frequently, thus are not suitable for addressing the short-term and frequent problems caused by DC piles. In this case, the VSCs can be adopted coordinately to further refine the voltage issues by their fast and flexible active and reactive power regulation capabilities. Moreover, the regulation of VSCs that are interconnected between the AC and DC lines can also alleviate the overloads and unbalance issues. Therefore, a coordinated control method of VSCs and OLTC for hybrid AC/DC LVDNs is proposed to comprehensively improve overloads, voltage violations, and unbalance issues caused by the AC and DC charging piles.

In the hybrid AC/DC LVDN, the converters at the terminal of DC lines are in the V_{dc}-Q control mode to establish the DC voltage, such as the VSC1 in Fig. 2 (b). The converters for interconnecting the AC and DC lines are in the P-Q control mode, such as the VSC2 and the VSC3 in Fig. 2 (b). Through active and reactive power control of VSC2 and VSC3, power transfer between interconnected lines can be realized to

alleviate the overloads of the DT and therefore avoid the three-phase unbalance and voltage violation problems. The proposed control method aims at optimizing the reference values of the active and reactive power of the VSCs to alleviate the multiple problems caused by EV charging, which is effective in presence of several numbers of VSCs with different specifics. Considering the limited communication within the LVDNs, the control strategy can be divided into two types: with communication and without communication. A control strategy without communication means that, VSC2 and VSC3 can measure only the local data and adjust their active and reactive power according to the local voltages. On the other hand, if communications are considered, VSC2 and VSC3 will communicate with the DT as well as the important nodes of the line, then adjust their active and reactive power according to the power of the DTs and the voltage of the communicable nodes.

The distribution system operator (DSO) is responsible for executing the proposed adaptive control of VSC and OLTC in a hybrid AC/DC LVDN. The active and reactive powers of VSCs and OLTCs are controlled by the proposed method in order to alleviate the multiple problems caused by EV charging, in which the EV charging power is determined by the EV owners' requirement and is not dispatched by the DSO. Note that the VSCs controlled in this paper are the interconnected VSCs between AC and DC lines (such as VSC2 and VSC3 in Fig. 2(b)), not the VSCs of EV owners.

In this section, firstly, the VSC control strategies aimed at alleviating the overload of the DTs, voltage violations, and three-phase unbalance are designed separately in Section III-A, III-B, and III-C. Then, a coordinated adaptive control strategy of OLTC and VSCs is proposed considering the simultaneous occurrence of multiple power quality issues in hybrid AC/DC LVDNs in Section III-D.

A. Alleviating the Overloads of DT by VSC

Considering that the formulated hybrid AC/DC LVDN has communications, then the VSC can obtain the three-phase active power measurements of DT. Therefore, overloads of DT can be alleviated by adjusting the three-phase active power of the VSC, which can be achieved as follows:

$$\Delta P_{\varphi}^{VSC}=\begin{cases}-(P_{\varphi}^{DT}-P_{DT}^{max}) & ,P_{\varphi}^{DT}>P_{DT}^{max}\\ 0 & ,P_{DT}^{min}<P_{\varphi}^{DT}<P_{DT}^{max}\\ -(P_{\varphi}^{DT}-P_{DT}^{min}) & ,P_{\varphi}^{DT}<P_{DT}^{min}\end{cases} \tag{6}$$

where ΔP_{φ}^{VSC} is the φ-phase active power adjustment, P_{φ}^{DT} is the measured active power at the terminal of the DT, P_{DT}^{max} and P_{DT}^{min} are the maximum and minimum power of the DT, respectively.

B. Eliminating the Voltage Violations by VSCs

As in LVDNs, the *R/X* ratio is larger than that in high-voltage transmission networks, the node voltage in LVDNs is sensitive not only to reactive power but also to active power. Therefore, both the active and reactive power can be used to regulate voltages. Considering the limited computing capability of LVDNs, the voltage sensitivity method can be used to achieve rapid voltage regulation. As a result, the hybrid AC/DC LVDN is decoupled into AC and DC parts by a VSC, and the AC part can be controlled by the three-phase four-wire voltage sensitivity method.

The voltage regulation on the AC-side of the VSC is:

$$[\Delta V^{AC}]=[S^{V-P}]\cdot[\Delta P_{VSC}^{AC}]+[S^{V-Q}]\cdot[\Delta Q_{VSC}^{AC}] \tag{7}$$

where ΔV^{AC} is the voltage deviation between the measured voltage and the upper or lower voltage limit on the AC-side, $S^{V\text{-}P}$ and $S^{V\text{-}Q}$ are the sensitivities between a measuring node and the VSC, and ΔP_{VSC}^{AC} and ΔQ_{VSC}^{AC} are respectively the real and reactive power adjustments of the VSC on the AC-side.

The voltage regulation equation on the DC side is:

$$[\Delta V^{DC}]=[S^{V-P}]\cdot[\Delta P_{VSC}^{DC}] \tag{8}$$

where ΔV^{DC} is the voltage deviation between the measured voltage and the upper or lower voltage limit on the DC side, and ΔP_{VSC}^{DC} is the real power adjustment of the VSC on the DC side.

The real power adjustment of the VSC on the AC-side and DC side needs to satisfy the following equation:

$$\Delta P_{VSC}^{AC}=-\Delta P_{VSC}^{DC} \tag{9}$$

If an AC node voltage exceeds the limits, the reactive power of the VSC is first considered to regulate the voltage, since the DC line is not affected by the reactive power regulation of the AC-side. Equation (10) is used to preliminarily calculate the three-phase adjustment of the reactive power $\Delta Q_{VSC,\varphi}^{AC}$.

$$\Delta Q_{VSC,\varphi}^{AC}=\Delta V_{i,\varphi}^{AC}\,/\,S_{i\varphi,VSC}^{V-Q} \tag{10}$$

where $\Delta V_{i,\varphi}^{AC}$ is the voltage deviation between the φ-phase voltage of node i and the upper or lower voltage limits. The upper and lower limits of the AC-side voltage are taken as 1.07 and 0.90 p.u., respectively. $S_{i,\varphi,VSC}^{V\text{-}Q}$ is the three-phase four-wire voltage sensitivity between node i and the VSC, which can be calculated using the perturbation and observation method [27].

If the reactive power adjustment $\Delta Q_{VSC,\varphi}^{AC}$ cannot be achieved due to the power rating limit of VSC, both active and reactive power are used to regulate node voltages.

$$\begin{cases}S_{i\varphi,VSC}^{V-P}\cdot\Delta P_{VSC,\varphi}^{AC}+S_{i\varphi,VSC}^{V-Q}\cdot\Delta Q_{VSC,\varphi}^{AC}=\Delta V_{i,\varphi}^{AC}\\ (P_{VSC}^{AC}+\Delta P_{VSC,\varphi}^{AC})^2+(Q_{VSC}^{AC}+\Delta Q_{VSC,\varphi}^{AC})^2=S_{max}^{VSC}\end{cases} \tag{11}$$

where S_{max}^{VSC} is the rated capacity of the VSC.

To reduce the impact on the DC side, the active power adjustment of VSCs should be as small as possible. The specific realization process of (11) is to gradually reduce the absolute value of the VSC's active power. $\Delta Q_{VSC,\varphi}^{AC}$ takes the maximum value that meets the capacity constraint until the voltage meets the constraint $0.9\le V_{i,\varphi}\le 1.07$.

If a DC node voltage exceeds the limits, real power is used to regulate node voltages based on (12). If the active capacity is insufficient, the active capacity is released by reducing the absolute value of the reactive power. At this time, the VSC's active and reactive power is adjusted according to (13).

$$\Delta P_{VSC}^{DC}=\Delta V_{j}^{DC}\,/\,S_{j,VSC}^{V-P} \tag{12}$$

$$\begin{cases}\Delta P_{VSC}^{AC}=-\Delta P_{VSC}^{DC}\\ \sqrt{(P_{VSC}^{AC}+\Delta P_{VSC,\varphi}^{AC})^2+(Q_{VSC}^{AC}+\Delta Q_{VSC,\varphi}^{AC})^2}=S_{max}^{VSC}\end{cases} \tag{13}$$

where ΔV_{j}^{DC} is the voltage deviation between the voltage of

node j at the DC side and the upper or lower voltage limits. The upper and lower limits of the DC side voltage are taken as 1.07 and 0.93 p.u., respectively. $S_{j,VSC}^{V\text{-}P}$ is the voltage sensitivity between node j and the VSC. There are two solutions for (13). To reduce the impact on the AC-side, the solution with the smaller $\Delta Q_{VSC,\varphi}^{AC}$ is used.

For LVDNs without communications, ΔV in (7)-(13) denotes the voltage overlimit deviation of the nodes connected to the AC and DC sides of the VSC. For networks with communications, ΔV is the maximum voltage overlimit deviation measured by the VSC.

C. Improving the Three-Phase Unbalance by VSC

The three-phase voltage unbalance factor (VUF) of the LVDNs is defined as follows [28]-[29]:

$$VUF_i = \max(\left|V_{i,\varphi} - V_i^{avr}\right| / V_i^{avr}) \times 100\%, \varphi \in \{a,b,c\} \tag{14}$$

where VUF_i is the voltage unbalance factor of node i, $V_{i,\varphi}$ and V_i^{avr} are respectively the φ-phase voltage and average voltage of node i and $V_i^{avr}=(V_{i,a}+V_{i,b}+V_{i,c})/3$.

If the VUF_i exceeds the upper limit (2% [30] used in this paper), the three-phase voltage is adjusted to the average voltage of node i by adjusting the power of the VSC to achieve voltage balance. The voltage sensitivity method is also used here. To reduce the impact on the DC side, the reactive power is first adjusted according to (10). If the reactive capacity is insufficient, (11) is used to achieve the coordinated control of active and reactive power.

Note that in the VSC control process for improving the three-phase unbalance, $\Delta V_{i,\varphi}^{AC}$ in (7)-(13) is the voltage deviation between the φ-phase voltage and average voltage of node i, i.e., $\Delta V_{i,\varphi}^{AC} = V_{i,\varphi}^{AC} - V_i^{avr}$.

For LVDNs without communications, $\Delta V_{i,\varphi}^{AC}$ is the voltage unbalance deviation of the nodes connected to the AC-side of the VSC. For networks with communications, $\Delta V_{i,\varphi}^{AC}$ is the maximum voltage unbalance deviation measured by the VSC.

D. Coordinated Adaptive Control Method of OLTC and VSCs

As the OLTC can help improve the voltage violations on long-time scale caused by AC piles, it can be coordinated with the VSC fast power control methods.

The regulation principle of the OLTC is as follows. The first step is to determine the period for OLTC adjustment. The load curve is divided into N_T periods according to the maximum number of tap adjustment in one day. Then, the second step is to calculate the tap position for each time period, which is determined based on the maximum voltage deviation and voltage sensitivity during the period. The tap position for the period N_t can be calculated by the sensitivity of node voltage to transformer ratio [28]. The tap position must be an integer and less than the maximum number of taps.

$$T_{tap}^{Nt} = \begin{cases} +[\dfrac{V_i - V_{max}}{S_i^{Vk} \cdot \Delta k}], & V_i > V_{max} \\ 0, & V_{min} \le V_i \le V_{max} \\ -[\dfrac{V_{min} - V_i}{S_i^{Vk} \cdot \Delta k}], & V_i \le V_{min} \end{cases} \tag{15}$$

where V_i is the voltage of node i, S_i^{Vk} is sensitivity of node voltage V_i to ratio of OLTC, Δk is the transformer ratio change per tap, V_{max} and V_{min} are the allowable maximum and minimum voltage, $[\cdot]$ represents the rounding function.

For the regulation sequence of OLTC and VSCs, the tap position of the OLTC in each period is determined first, and then the power of the VSC is regulated according to the measured node voltages and DT power at each moment. For the simultaneous occurrence of multiple power quality issues, the VSC power control strategies are carried out in sequence of alleviating the overloads of DT, eliminating the voltage violations and improving the three-phase unbalance. The implementation flowchart of the proposed coordinated control method of OLTC and VSCs is shown in Fig. 4, and the detailed steps are as follows.

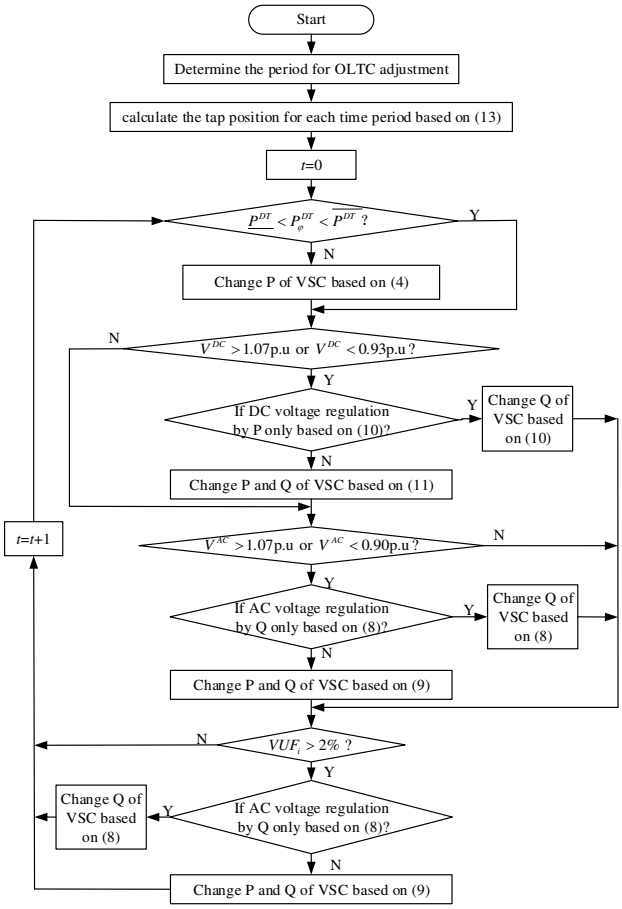

Fig. 4. Flowchart of the proposed control strategy.

Step 1: determine the period for OLTC adjustment and calculate the tap position for each time period.

Step 2: measure the node voltages and the output power of the DT at each time t.

Step 3: judge if the issue of overload, voltage violation, or three-phase unbalance occurs, then calculate the reference values of VSC active and reactive power according to the proposed control methods.

Step 4: adjust the VSC active and reactive power according to the calculated reference values.

IV. Case Studies

Two case studies are conducted in this section by numerical simulation. In Section IV. A, one of the three AC lines is converted to DC operation, which is used to demonstrate the advantages of DC conversion in reducing voltage deviation, increasing power transfer capacity, and accommodating EVs. In Section IV. B, a 5-feeder hybrid AC/DC LVDN is utilized to demonstrate the effectiveness of the proposed control strategy in improving overloads, voltage violations, and three-phase unbalance.

A. Case Study 1: Advantages of DC Conversion

The LVDN topology under study is modified from [29], shown previously as Fig. 2(a), where the distribution area of DT1 consists of three lines, marked as Line-1, Line-2 and Line-3, respectively. The type of conductor is LGJ-50, and the capacity of the DT is 400 kVA in case study. The voltage regulation range of the OLTC is ±2×2.5% and maximum number of tap adjustment in one day is 5 times. The maximum transfer capacity of the AC LVDN is 390 kW, i.e., 130 kW for each line. The locations of PV generations and EV charging piles in the hybrid AC/DC LVDNs are shown in Fig. 2(b). The rated power of single-phase PV generation is 6 kW, the charging power of a single-phase AC pile is 7 kW, and that of a DC pile is 40 kW. The length of each branch shown in Fig. 2(a) is 50 m, and the impedance parameter of three-phase four-wire LV line is Z_0. Moreover, the simulation software used in this paper is MATLAB R2016a.

$$Z_0 = \begin{bmatrix} 0.6500+j0.4120 & 0.0065+j0.0041 & 0.0065+j0.0041 & 0.0065+j0.0041 \\ 0.0065+j0.0041 & 0.6500+j0.4120 & 0.0065+j0.0041 & 0.0065+j0.0041 \\ 0.0065+j0.0041 & 0.0065+j0.0041 & 0.6500+j0.4120 & 0.0065+j0.0041 \\ 0.0065+j0.0041 & 0.0065+j0.0041 & 0.0065+j0.0041 & 0.6500+j0.4120 \end{bmatrix}$$

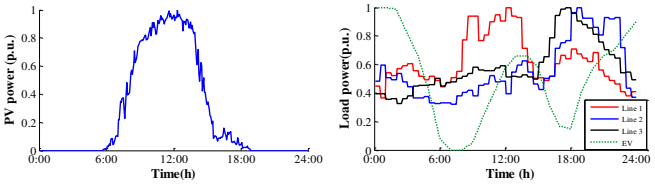

Fig. 5. Power curves of PVs and loads.

The proposed DC conversion scheme is to convert Line-3 into DC operation to form a hybrid AC/DC LVDN, where the PV generation and DC charging piles in Line-1 and Line-2 are integrated into Line-3. According to the analysis in Section II. B, the parallel operation monopole is adopted. The 24-h power curves of loads and PVs are shown in Fig. 5, and the sampling interval of the load and PV data is 5 min.

The maximum and minimum voltages of the three lines within 24 h are shown in Fig. 6. Before DC conversion, undervoltage occurs in Line-1 at midday and night during the peak charging periods of EVs. After DC conversion, the voltage deviation is reduced due to the decrease in power flow in Line-1, as shown in Fig. 6 (a). For example, at 12:30, the power at the head of Line-1 in AC LVDN is 66.96 kW + j22.98 kVar, and the minimum voltage is 0.87 p.u. For the hybrid AC/DC LVDN, the power at the head of Line-1 is reduced to 50.52 kW + j20.84 kVar, and the minimum voltage is 0.91 p.u.

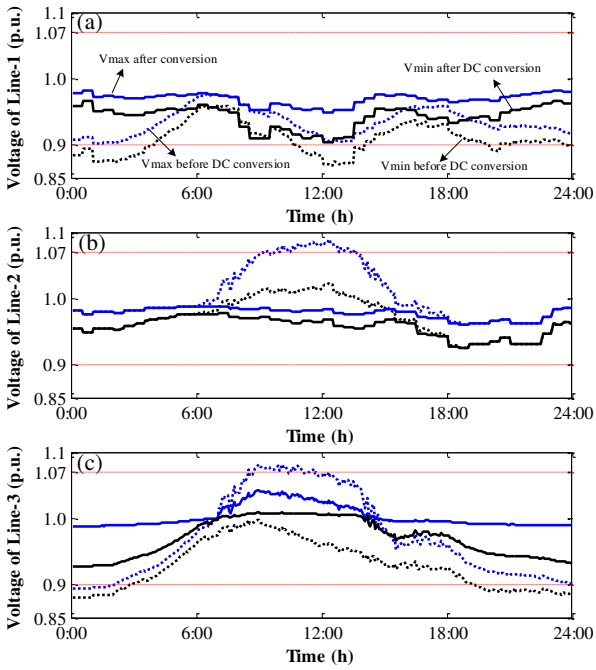

Fig. 6. Maximum and minimum voltages of the three lines.

As for the voltage of Line-2 in Fig. 6 (b), its maximum voltage deviation exceeds the upper limit during 9:50-13:40 in the AC LVDN. During this period, the reverse power flow is formed in the line due to the high PV output and low load demand, which leads to overvoltage. When overvoltage issues are the most severe at 12:20, the power at the head of the line is -55.01 kW + j8.37 kVar (the active power is the reverse power), and the maximum voltage of Line-2 is 1.09 p.u. After DC conversion, there is no reverse power flow in Line-2 in the hybrid AC/DC LVDN, and the voltage at each moment meets the voltage constraint.

As for the voltage of Line-3 in Fig. 6 (c), before DC conversion, the issues of overvoltage occur at midday and undervoltage occur at night. Although the power at the head of Line-3 increases after DC conversion, the voltage deviation of the DC network is smaller than that of the AC network, because the reactive power and reactance of the DC line are zero. For example, at 10:00, the active power at the head of Line-3 increases from 19 kW to 31 kW, but the maximum voltage decreases from 1.08 to 1.04 compared with the results of the AC network. Therefore, the voltages of Line-3 are in the secure range in the hybrid AC/DC LVDN.

The undervoltage and overvoltage issues of the three lines can also be improved by regulating the OLTC. The load curve is divided into 4 periods for OLTC adjustment, and the tap positions for each period are calculated by eq. (13). The regulation result of the OLTC is shown in Fig. 7.

During the first period (19:00-4:00), undervoltage issues occur in Line-1 and Line-3, and the tap of the OLTC is regulated to -2.5%. The undervoltage issues in the network are thus alleviated with the proper tap adjustment. The minimum voltage is 0.90 p.u. in Line-1.

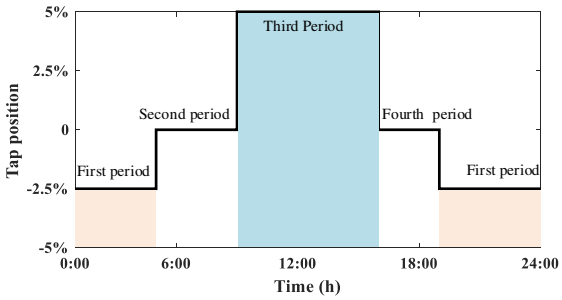

Fig. 7. Regulation result of the OLTC.

During the second and fourth periods, there is on undervoltage or over voltage issues occur in the three lines. Therefore, the tap of the OLTC is regulated to zero.

During the third period (9:00-15:00), undervoltage issues occur in Line-1, while overvoltage issues occur in Line-2 and Line-3. In order to improve the voltage of the whole network, the tap is adjusted up to +5%. The overvoltage issues in Line-2 and Line-3 are alleviated. However, the undervoltage issues of line 1 are aggravated, and the minimum voltage is 0.83 p.u.

Therefore, for scenarios where overvoltage and undervoltage issues occur at the same time, OLTC can only improve one voltage issue. In the hybrid AC/DC LVDNs, the VSC can be further regulated to completely eliminate the voltage issues.

Assuming that the load power at all nodes increases at the same rate, the maximum transfer capability of the AC LVDN is approximately 190 kW when the lowest node voltage reaches 0.93 p.u., which is far below the AC line transfer capacity as 390 kW. In the hybrid AC/DC network, the maximum transfer capability is increased to approximately 320 kW, which is 1.68 times that of the AC network.

Due to the lower voltage deviation and larger transfer capability of the DC network, the maximum EV penetration of the hybrid AC/DC LVDN is increased from 85% to 215% compared with the AC LVDN, as shown in Fig. 8. Therefore, the advantages of the proposed DC conversion method have been verified.

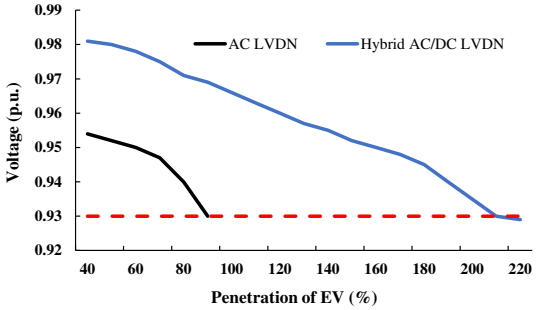

Fig. 8. Voltages under different EV penetrations.

B. Case Study 2: Superiority of the Proposed Adaptive Control Strategy of Hybrid AC/DC LVDN

To further verify the effectiveness of the proposed coordinate control strategy for hybrid AC/DC LVDNs, two AC lines (marked as Line-4 and Line-5) are added to realize the interconnection of AC and DC lines based on *Case Study 1*, as shown in Fig. 2(b). The capacity of DT2 and DT3 is 100 kVA, and the allowable range of the DT load rate is [-60%, +80%]. PV and load power variations during 9:00-15:00, as shown in Fig. 9, are used to test the effectiveness of the proposed control strategy. It is assumed that VSC2 and VSC3 measure the node voltages and change the power output every 5 min. The tap position of the OLTC is adjusted up to +5% during this period according to Fig. 7.

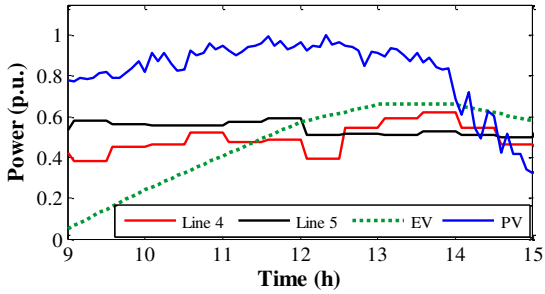

Fig. 9. Loads and PV outputs from 9:00 to 15:00.

Four cases are compared in this section: 1) the base case without any control, 2) the control strategy for voltage violation issues, 3) the control strategy for unbalance issues, and 4) the proposed coordinated control strategy for multiple issues. In Fig. 10, the results of three-phase voltage deviations in the four cases are presented, assuming that the LVDN has communication.

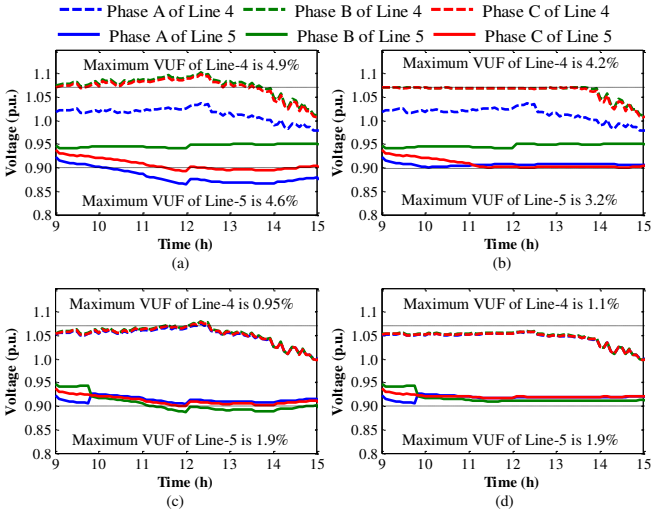

Fig. 10. Voltage deviations. (a) Base case. (b) Control strategy for voltage violation. (c) Control strategy for unbalance; (d) Proposed coordinated control strategy.

For the base case as *Case 1*, the B-phase and C-phase voltages of Line-4 violate the permitted upper limit from 9:00 to 13:40, and the VUF exceeded the allowable limit during 9:00-15:00 due to the high penetration of PVs in phases B and C, as shown by the dotted line in Fig. 10 (a). The maximum voltage deviation and VUF of Line-4 are 1.12 p.u. and 4.9%, respectively. The undervoltage issues occur in phases A and B of Line-5 during 9:00-15:00, and unbalance issues occur from 9:50 to 15:00 because of the unbalanced load and single-phase AC charging piles of EVs, as shown by the solid line in Fig. 10 (a). The maximum voltage deviation and VUF of Line-5 are 0.86 p.u. and 4.6%, respectively. Moreover, the maximum

B-phase and C-phase reverse power of DT2 is 75 kW and 80 kW, which exceed the allowable limit of 60%. The maximum load rate of DT3 reaches 85% in phase A, which exceeds the allowable limit of 80%.

For *Case 2* with the control strategy for voltage violation in Fig. 10 (b), the overvoltage and undervoltage issues can be eliminated. For more insights, the power of VSC2 and VSC3 that injected into the AC-side under this control is presented in Fig. 11. As shown in Fig. 11 (a) by the dotted line, the B-phase and C-phase reactive power of VSC2 is absorbed from the AC-side, while the B-phase and C-phase reactive power at the head of Line 4 is increased due to the reactive power of VSC2, as shown in Fig. 11 (a) by the solid line. Therefore, the B-phase and C-phase voltages of Line 4 decrease. At the same time, the A-phase and C-phase power at the head of Line 5 is reduced because the A-phase and C-phase reactive power of VSC3 is injected into the AC-side, as shown in Fig. 11 (b). Therefore, the undervoltage problem of Line 5 caused by EVs is eliminated. Although the reactive power of VSC2 and VSC3 alleviates the three-phase unbalance in this case, the maximum VUF (4.2% in Line-4 and 3.2% in Line-5) still exceeds the limit of 2%, which needs extra control for the unbalance issue.

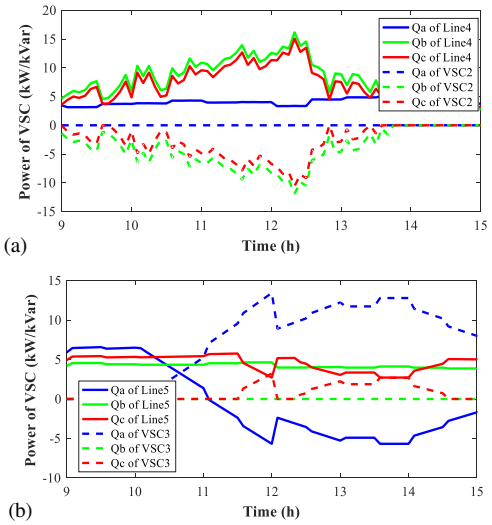

Fig. 11. Power of VSCs injected into the AC side under the control strategy for voltage violation. (a) VSC2; (b) VSC3.

For *Case 3* with the control strategy for three-phase unbalance, as shown in Fig. 10 (c), the VUF is greatly reduced (0.95% in Line-4 and 1.9% in Line-5). For more insights, the power of VSC2 and VSC3 that injected into the AC-side under this control is presented in Fig. 12. As shown in Fig. 12 by the dotted line, the B-phase and C-phase reactive power of VSC2 is absorbed from the AC-side, while the A-phase reactive power is injected into the AC-side. The amplitude of the three-phase voltage tends to be constant because of the reactive power of VSC2. However, this strategy worsens the C-phase voltage, resulting in the normal C-phase voltage exceeding the upper limit during 12:00-12:30. The same situation occurs in Line-5. The VUF of Line-5 is reduced due to the reactive power of VSC3, in which A-phase and B-phase power is injected into the AC-side, and C-phase power is absorbed from the AC-side, as shown in Fig. 12 by the solid line. However, the regulation of the reactive power of VSC3 leads to voltage violation in phase B that requires extra control.

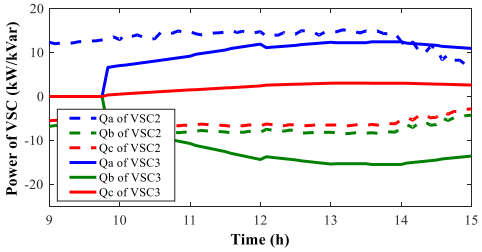

Fig. 12. Power of VSCs injected into the AC side under the control strategy for three-phase unbalance.

For *Case 4* with the proposed coordinated control strategy, the overloads of DT2 and DT3 are alleviated by the active power of the VSC. As shown in Fig. 13 (a), the reverse power of DT2 after control is in the allowable limit, since the B-phase and C-phase active power of VSC2 is absorbed from the AC-side. The load rate of DT3 in phase A after control is less than 80% because the A-phase active power of VSC3 is injected into the AC-side, as shown in Fig. 13 (b).

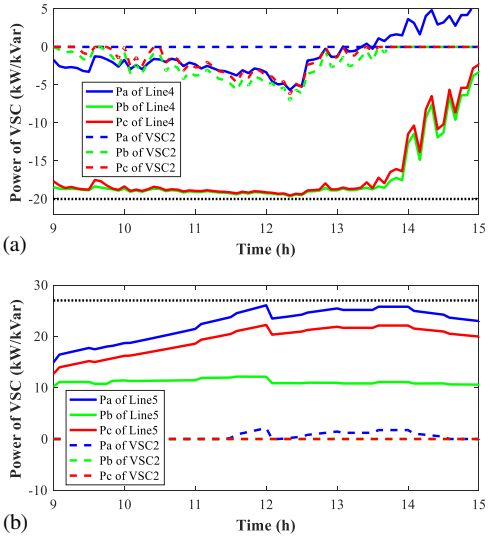

Fig. 13. Active power of VSCs injected into the AC side under the proposed coordinated control strategy. (a) VSC2; (b) VSC3.

Besides, as shown in Fig. 10 (d), the voltage violation and unbalance issues are both eliminated with the proposed coordinated control strategy. Similarly, the power of VSC2 and VSC3 that injected into the AC-side under this control is presented in Fig. 14. As shown in Fig. 14 (a), the B-phase and C-phase reactive power of VSC2 is absorbed from the AC-side, while the A-phase reactive power is injected into the AC-side. Therefore, the B-phase and C-phase voltages of Line-4 decreases, the A-phase voltage increases, and the three-phase voltages tend to be equal. In the same way, the three-phase voltages of Line-5 are balanced and do not exceed the limit, as the A-phase and C-phase reactive power of VSC3 is injected into the AC-side, while the B-phase reactive power is absorbed from the AC-side, as shown in Fig. 14 (b).

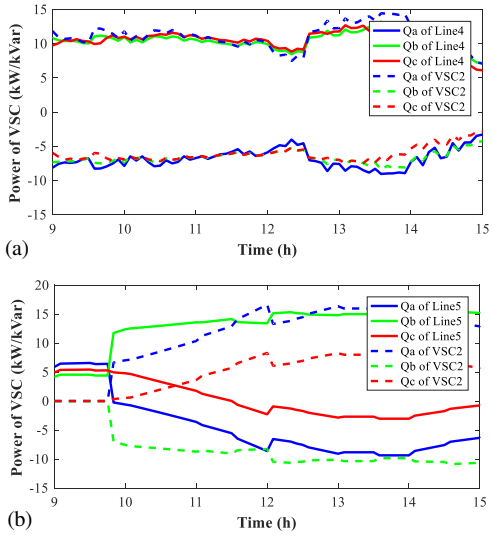

Fig. 14. Reactive power of VSCs injected into the AC side under the proposed coordinated control strategy. (a) VSC2; (b) VSC3.

According to the results in Fig. 10 (b)-(d), it is demonstrated that the proposed strategy can realize a comprehensive improvement of overload, voltage violation and three-phase unbalance issues. Compared with the separate control strategy for voltage violation or three-phase unbalance, the proposed adaptive multi-mode control strategy can not only ensure that the three-phase voltages do not exceed the limit, but also eliminates the three-phase unbalance, which does not degrade the original normal voltage.

The operating indexes of the proposed coordinated control strategy for multiple issues with and without communication are shown in Table II. In the case without communication, the maximum voltage, minimum voltage, maximum VUF and power losses are 1.08, 0.88, 2.5% and 60.32 kWh, respectively. The node voltages and power losses are improved compared with the base case thanks to the power regulation of the VSC2 and VSC3. However, voltage violations and unbalance issues are not completely eliminated in this case, since the active and reactive power of the VSCs is adjusted according to the voltage measurement of the nodes connected to the VSCs (i.e., node 8 of Line-4 and Line-5), which cannot represent the most severe situation of the LVDNs. In the case with communication, the voltage violations and unbalance issues are completely improved, since the VSC2 and VSC3 can measure the voltages of all nodes and control their power according to the most severely affected nodes to improve the power quality issues. Moreover, the power losses in this case are further reduced to 54.35 kWh.

TABLE II
OPERATING INDEXES UNDER DIFFERENT STRATEGIES

Cases	V_{max}	V_{min}	VUF_{max}	P_{loss} (kWh)
Base case	1.12	0.86	4.9%	80.54
Without communication	1.08	0.88	2.5%	60.32
With communication	1.06	0.90	1.9%	54.35

V. CONCLUSIONS

This paper proposes EV integration-oriented DC conversion schemes for three-phase four-wire LVDNs and the associated control strategy, which can alleviate the multiple problems caused by EV charging piles, release more capability for EVs and further promote the transportation electrification.

Based on the proposed DC conversion scheme, a hybrid AC/DC LVDN is formed by converting some of the existing AC lines in a distribution network to DC operation. Through the DC conversion, the capacities of distribution lines can be increased. As a result, the maximum EV penetration of the hybrid AC/DC LVDN is increased from 85% to 215% compared with the results of the AC LVDN, which benefits from the smaller voltage deviation and larger transfer capability of the DC circuits.

An adaptive control strategy is also proposed considering the simultaneous occurrence of overload, voltage violations, and three-phase unbalance issues in hybrid AC/DC LVDNs with EVs. Three-phase active and reactive power of VSCs are coordinately utilized to improve the power flow without causing degradation of the original normal voltages.

REFERENCES

[1] A. Haxhiu, A. Abdelhakim, S. Kanerva and J. Bogen, "Electric Power Integration Schemes of the Hybrid Fuel Cells and Batteries-Fed Marine Vessels—An Overview," *IEEE Trans. Transport. Electrific.*, vol. 8, no. 2, pp. 1885-1905, June 2022.

[2] A. Navarro-Espinosa and L. F. Ochoa, "Probabilistic Impact Assessment of Low Carbon Technologies in LV Distribution Systems," *IEEE Trans. Power Syst.*, vol. 31, no. 3, pp. 2192-2203, May 2016.

[3] M. A. Azzouz, M. F. Shaaban and E. F. El-Saadany, "Real-Time Optimal Voltage Regulation for Distribution Networks Incorporating High Penetration of PEVs," *IEEE Trans. Power Syst.*, vol. 30, no. 6, pp. 3234-3245, Nov. 2015.

[4] Q. Hu, S. Bu and V. Terzija, "A Distributed P and Q Provision-Based Voltage Regulation Scheme by Incentivized EV Fleet Charging for Resistive Distribution Networks," *IEEE Trans. Transport. Electrific.*, vol. 7, no. 4, pp. 2376-2389, Dec. 2021.

[5] J. Su, T. T. Lie and R. Zamora, "Integration of Electric Vehicles in Distribution Network Considering Dynamic Power Imbalance Issue," *IEEE Trans. Ind. Appl*, vol. 56, no. 5, pp. 5913-5923, Sept.-Oct. 2020.

[6] O. Hafez and K. Bhattacharya, "Queuing Analysis Based PEV Load Modeling Considering Battery Charging Behavior and Their Impact on Distribution System Operation," *IEEE Trans. Smart Grid*, vol. 9, no. 1, pp. 261-273, Jan. 2018.

[7] Q. Dai, T. Cai, S. Duan and F. Zhao, "Stochastic Modeling and Forecasting of Load Demand for Electric Bus Battery-Swap Station," *IEEE Trans. Power Deliv.*, vol. 29, no. 4, pp. 1909-1917, Aug. 2014.

[8] L. Sun and D. Lubkeman, "Agent-Based Modeling of Feeder-Level Electric Vehicle Diffusion for Distribution Planning," *IEEE Trans. Smart Grid*, vol. 12, no. 1, pp. 751-760, Jan. 2021.

[9] A. Dubey and S. Santoso, "Electric vehicle charging on residential distribution systems: Impacts and mitigations," *IEEE Access*, vol. 3, pp. 1871–1893, 2015.

[10] C. Sabillon-Antunez, O. D. Melgar-Dominguez, J. F. Franco, M. Lavorato and M. J. Rider, "Volt-VAr Control and Energy Storage Device Operation to Improve the Electric Vehicle Charging Coordination in Unbalanced Distribution Networks," *IEEE Trans. Sustain. Energy*, vol. 8, no. 4, pp. 1560-1570, Oct. 2017.

[11] G. E. Mejia-Ruiz, R. Cárdenas-Javier, M. R. Arrieta Paternina, J. R. Rodríguez-Rodríguez, J. M. Ramirez and A. Zamora-Mendez, "Coordinated Optimal Volt/Var Control for Distribution Networks via D-PMUs and EV Chargers by Exploiting the Eigensystem Realization," *IEEE Trans. Smart Grid*, vol. 12, no. 3, pp. 2425-2438, May 2021.

[12] T. Stetz, F. Marten and M. Braun, "Improved Low Voltage Grid-

Integration of Photovoltaic Systems in Germany," *IEEE Trans. on Sustain. Energy*, vol. 4, no. 2, pp. 534-542, April 2013.

[13] H. M. A. Ahmed, A. B. Eltantawy and M. M. A. Salama, "A planning approach for the network configuration of AC-DC hybrid distribution systems," *IEEE Trans. Smart Grid*, vol. 9, no. 3, pp. 2203-2213, May 2018.

[14] J. Yu, K. Smith, M. Urizarbarrena, N. MacLeod, R. Bryans, and A. Moon, "Initial designs for the ANGLE DC project; converting existing AC cable and overhead line into DC operation," *in 13th IET International Conference on AC and DC Power Transmission (ACDC 2017)*, Manchester, UK, 2017, pp. 1-6.

[15] X. Liu, P. Wang and P. C. Loh, "A hybrid AC/DC microgrid and its coordination control," *IEEE Trans. Smart Grid*, vol. 2, no. 2, pp. 278-286, Jan. 2011.

[16] G. Abeynayake, G. Li, T. Joseph, J. Liang, and W. Ming, "Reliability and cost-oriented analysis, comparison and selection of multi-level MVDC converters," *IEEE Trans. Power Delivery*, vol. 36, no. 6, pp. 3945-3955, Dec. 2021.

[17] S. K. Chaudhary, J. M. Guerrero and R. Teodorescu, "Enhancing the capacity of the AC distribution system using DC interlinks—a step toward future DC grid," *IEEE Trans. Smart Grid*, vol. 6, no. 4, pp. 1722-1729, July 2015.

[18] L. Zhang, J. Liang, W. Tang, G. Li, Y. Cai, and W. Sheng, "Converting AC distribution lines to DC to increase transfer capacities and DG penetration," *IEEE Trans. Smart Grid*, vol. 10, no. 2, pp. 1477-1487, March 2019.

[19] A. Shekhar, L. M. Ramirez-Elizondo, T. B. Soeiro, and P. Bauer, "Boundaries of operation for refurbished parallel AC-DC reconfigurable links in distribution grids," *IEEE Trans. Power Delivery*, vol. 35, no. 2, pp. 549-559, April 2020.

[20] A. A. Eajal, M. F. Shaaban, K. Ponnambalam and E. F. El-Saadany, "Stochastic Centralized Dispatch Scheme for AC/DC Hybrid Smart Distribution Systems," *IEEE Trans. Sustain. Energy*, vol. 7, no. 3, pp. 1046-1059, July 2016.

[21] L. Zhang, B. Tong, Z. Wang, W. Tang and C. Shen, "Optimal Configuration of Hybrid AC/DC Distribution Network Considering the Temporal Power Flow Complementarity on Lines," *IEEE Trans. Smart Grid*, vol. 13, no. 5, pp. 3857-3866, Sept. 2022.

[22] F. Qiao and J. Ma, "Coordinated voltage/var control in a hybrid AC/DC distribution network," *IET Generation, Transmission & Distribution*, vol. 14, pp. 2129-2137, 2020.

[23] H. Jia, Q. Xiao and J. He, "An Improved Grid Current and DC Capacitor Voltage Balancing Method for Three-Terminal Hybrid AC/DC Microgrid," *IEEE Transactions on Smart Grid*, vol. 10, pp. 5876-5888, 2019.

[24] Y. Fu, Z. Zhang, Z. Li, and Y. Mi, "Energy Management for Hybrid AC/DC Distribution System With Microgrid Clusters Using Non-Cooperative Game Theory and Robust Optimization," *IEEE Transactions on Smart Grid*, vol. 11, pp. 1510-1525, 2020.

[25] L. Zhang, C. Zhao, B. Zhang, G. Li, and W. Tang, "Voltage control method based on three-phase four-wire sensitivity for hybrid AC/DC low-voltage distribution networks with high-penetration PVs," *IET Renewable Power Generation*, vol. 16, pp. 700-712, 2022.

[26] T. Chen, X. Zhang, J. Wang, J. Li, C. Wu, M. Hu, and H. Bian, "A Review on Electric Vehicle Charging Infrastructure Development in the UK," *Journal of Modern Power Systems and Clean Energy*, vol. 8, pp. 193-205, March 2020.

[27] F. Tamp and P. Ciufo, "A sensitivity analysis toolkit for the simplification of mv distribution network voltage management," *IEEE Trans. Smart Grid*, vol. 5, no. 2, pp. 559-568, March 2014.

[28] P. Wang, D. H. Liang, J. Yi, P. F. Lyons, P. J. Davison and P. C. Taylor, "Integrating Electrical Energy Storage into Coordinated Voltage Control Schemes for Distribution Networks," *IEEE Trans. Smart Grid*, vol. 5, no. 2, pp. 1018-1032, March 2014.

[29] W. Tang, Y. Cai, L. Zhang, B. Zhang, Z. Wang, Y. Fu, and X. Xiao, "Hierarchical coordination strategy for three-phase MV and LV distribution networks with high-penetration residential PV units," *IET Renewable Power Generation*, vol. 14, pp. 3996-4006, 2020.

[30] A. O'Connell and A. Keane, "Volt–var curves for photovoltaic inverters in distribution systems," *IET Gener. Transm. Distrib.*, vol. 11, no. 3, pp. 730-739, Feb. 2017.